$\mathcal{O}(\alpha_s)$ corrections to $e^+e^- \to J/\psi + \eta_{c2}(\chi'_{c1})$ at B factories

Hai-Rong Dong,[1,*] Feng Feng,[2,3,†] and Yu Jia[1,3,4,‡]

[1]*Institute of High Energy Physics and Theoretical Physics Center for Science Facilities, Chinese Academy of Sciences, Beijing 100049, China*
[2]*China University of Mining and Technology, Beijing 100083, China*
[3]*Center for High Energy Physics, Peking University, Beijing 100871, China*
[4]*School of Physics, University of Chinese Academy of Sciences, Beijing 100049, China*

(Received 9 January 2013; published 6 August 2018)

We investigate the $\mathcal{O}(\alpha_s)$ correction to $e^+e^- \to J/\psi + \eta_{c2}$ in the NRQCD factorization approach. A detailed comparative study between $e^+e^- \to J/\psi + \eta_{c2}$ and $e^+e^- \to J/\psi + \chi'_{c1}$ at the B factory energy is also carried out. After incorporating the $\mathcal{O}(\alpha_s)$ correction, we predict the cross section for the former process to be around 0.3 fb, while that of the latter is about 6 times greater. The outgoing J/ψ is found to be dominantly transversely polarized in the former process, while longitudinally polarized in the latter. These features may provide valuable guidance for the Belle 2 experiment to establish the χ'_{c1} or η_{c2} states. In the Appendix, we also identify the coefficients of the double logarithms of form $\ln^2(s/m_c^2)$ associated with all the relevant next-to-leading-order Feynman diagrams, for the helicity-suppressed double-charmonium production channels $e^+e^- \to J/\psi + \eta_{c2}$ and $e^+e^- \to J/\psi + \chi_{c0,1,2}$.

DOI: 10.1103/PhysRevD.98.034005

I. INTRODUCTION

Since a number of double charmonium production processes were first discovered at B factory more than a decade ago [1–3], this topic has spurred a widespread interest [4]. Firstly, this production environment provides a unique and powerful means to search for the new C-even charmonium states, especially those X, Y, Z states, by fitting the recoil mass spectrum against the J/ψ (ψ'). The most famous examples are the discovery of the $X(3940)$ [5] and the $X(4160)$ [6] by this way.

Another appealing reason to study double charmonium production is that it provides a new stage to sharpen our understanding toward perturbative QCD, especially toward the application of the light-cone approach [7,8] and the nonrelativistic QCD (NRQCD) factorization approach [9] to hard exclusive reactions involving heavy quarkonium.

The most famous double-charmonium production process is perhaps $e^+e^- \to J/\psi + \eta_c$. The original lowest-order (LO) NRQCD predictions to this process [10,11] is about 1 order of magnitude smaller than the measurement [1]. This alarming discrepancy has triggered a great amount of theoretical investigations in both NRQCD and light-cone approaches [12–22]. One crucial element in alleviating the discrepancy between the NRQCD prediction and the data is the substantial and positive next-to-leading-order (NLO) perturbative corrections [16,17]. By contrast, owing to some long-standing theoretical obstacles, the NLO correction to this helicity-suppressed process in the light-cone approach has never been successfully worked out [7,8]. As a consequence, despite some shortcomings, the NRQCD approach seems to be the only viable method which is based on the first principle and also systematically improvable.

Some time ago, the $\mathcal{O}(\alpha_s)$ corrections to the double-charmonium production processes which involves J/ψ plus a P-wave charmonium, e.g., $e^+e^- \to J/\psi + \chi_{c0,1,2}$ have also been investigated in the NRQCD approach [23,24]. For some production channels, the effect of the NLO perturbative corrections can be important.

In this work, we aim to carry out a comprehensive study of the NLO perturbative corrections to the processes $e^+e^- \to J/\psi + \eta_{c2}$ and $e^+e^- \to J/\psi + \chi'_{c1}$, again in the NRQCD factorization framework. The calculation for the former process, which involves associated production of J/ψ plus a D-wave charmonium, is new, while that for the latter can be readily adapted from Ref. [24]. This work should be considered as a sequel of Refs. [21,24].

Our interest in conducting such a comparative study was originally motivated by the controversy raised for the quantum number of the $X(3872)$ meson, whether it being 1^{++} or 2^{-+}, originally trigged by a *BABAR* paper in

*donghr@ihep.ac.cn
†F.Feng@outlook.com
‡jiay@ihep.ac.cn

Published by the American Physical Society under the terms of the Creative Commons Attribution 4.0 International license. Further distribution of this work must maintain attribution to the author(s) and the published article's title, journal citation, and DOI. Funded by SCOAP³.

2010 [25].[1] Consequently, the canonical charmonium options for the $X(3872)$ would be the χ'_{c1} and η_{c2}, respectively. After the unexpected *BABAR* results [25], there had arose a flurry of studies about critically distinguishing the properties of χ'_{c1} and η_{c2}, such as the radiative transitions $\eta_{c2}(\chi'_{c1}) \to J/\psi(\psi')\gamma$ [28–30], the $\eta_{c2}(\chi'_{c1})$ hadroproduction rates [31], or $\eta_{c2}(\chi'_{c1})$ production rates in B decay [32]. By confronting the established properties of $X(3872)$, all these studies tend to disfavor the $^1D_2$ assignment of the $X(3872)$ meson. Our hope was that double-charmonium production can also be added to the above list as a valuable means to help clarify the situation. Nevertheless, through a key analysis of angular distributions of dipions in $X(3872) \to J/\psi\pi^+\pi^-$ at LHCb in 2013 [27], the 2^{-+} assignment has been safely excluded, and the 1^{++} quantum number has been firmed established for the $X(3872)$ particle.

Although our original incentive now looks somewhat obsolete, it is still beneficial to carefully study the production rate of $J/\psi + \chi'_{c1}$ and $J/\psi + \eta_{c2}$. Firstly, due to the cleanness and efficiency of reconstructing J/ψ via its leptonic decay channel, the double charmonium production process at B factory remains to serve a competitive and appealing environment to establish the χ'_{c1} and η_{c2} states. It turns out that the production rate of $e^+e^- \to J/\psi + \chi'_{c1}$ is about 6–7 times greater than that of $e^+e^- \to J/\psi + \eta_{c2}$. Based on the 1 ab^{-1} data currently accumulated at the BELLE experiment, it looks promising to observe the former process, if the χ'_{c1} can indeed be regarded as the $X(3872)$ particle with very narrow width. Also, this production channel may also provide a clean way to search for the not-yet-observed η_{c2} state. These phenomenological considerations seem to constitute strong enough motivation for experimentalists to continue to serach the double charmonium production in the forthcoming Belle 2 experiments.

The rest of the paper is organized as follows. In Sec. II, we specify the helicity selection rule suited for the hard exclusive reaction $e^+e^- \to J/\psi + \eta_{c2}$, and give the definition for the dimensionless, reduced helicity amplitudes. In Sec. III, we present the leading-order expressions for all the independent helicity amplitudes in the NRQCD factorization framework. In Sec. IV, we first review some key technical issues about the $\mathcal{O}(\alpha_s)$ calculation, then present the asymptotic expressions for the NLO perturbative corrections to all the encountered helicity amplitudes. The pattern of the double-logarithmic scaling violation is confirmed once again. In Sec. V, a comparative study is performed for both unpolarized and polarized cross sections between the processes $e^-e^+ \to J/\psi + \eta_{c2}$ and $e^-e^+ \to J/\psi + \chi'_{c1}$. This study may shed some light on unveiling the quantum number of the $X(3872)$ meson in the future double-charmonium production experiments. Finally, we summarize in Sec. VI. In the Appendix, we tabulate the coefficients of the double logarithms $\ln^2(s/m_c^2)$ associated with all the relevant NLO Feynman diagrams, for all the double-charmonium production channels we have studied so far, i.e., $e^+e^- \to J/\psi + \eta_{c2}(\eta_c, \chi_{c0,1,2})$.

[1]Note the first version of this work was finished in January 2013 [26]. By that time, the η_{c2} option of the $X(3872)$ was still not yet fully excluded from experimental angle. The situation then drastically changed after the release of a LHCb paper in February 2013 [27].

II. HELICITY SELECTION RULE AND REDUCED HELICITY AMPLITUDES

It is often desirable to glean more information than simply present the unpolarized cross section for a hard exclusive reaction, especially for the double-charmonium production process considered in this work. It is of particular advantage to making explicit predictions to various $J/\psi + \eta_{c2}$ production rates for different helicity configurations. The underlying reasons of carrying out such detailed studies are two-fold. On the experimental ground, once the sufficient statistics is achieved, the helicity amplitudes themselves in principle can be measured by studying the angular distributions of these charmonia and their decay products; from the theoretical perspective, it is also instructive to stay with the helicity amplitudes. The reason is that, for a hard exclusive reaction, the relative importance of the polarized cross section in a given helicity channel is dictated by the celebrated *helicity selection rule* (HSR) [33].

We are interested in the hard-scattering limit $\sqrt{s} \gg m_c \gg \Lambda_{\rm QCD}$, where $\sqrt{s}$ stands for the center-of-mass energy of the e^+e^- collider, m_c for the charm quark mass, and $\Lambda_{\rm QCD}$ for the intrinsic QCD scale. In this limit, the asymptotic behavior of the production rate for $J/\psi + \eta_{c2}$ in a definite helicity configuration follows from the HSR [10]:

$$\frac{\sigma[e^+e^- \to J/\psi(\lambda_1) + \eta_{c2}(\lambda_2)]}{\sigma[e^+e^- \to \mu^+\mu^-]} \sim v^{10}\left(\frac{m_c^2}{s}\right)^{2+|\lambda_1+\lambda_2|}, \qquad (1)$$

where λ_1, λ_2 represent the helicities carried by the $J/\psi, \eta_{c2}$, respectively. v denotes the characteristic velocity of charm quark inside a charmonium. Equation (1) implies that the helicity state which exhibits the slowest asymptotic decrease, thus constitutes the "leading-twist" contribution, i.e., $\sigma \sim 1/s^3$, is $(\lambda_1, \lambda_2) = (0, 0)$.

We have chosen, by default, to work in the e^+e^- center-of-mass frame. Let $|\mathbf{P}|$ signify the magnitude of the momentum carried by the J/ψ (η_{c2}) and θ denote the angle between the moving directions of the J/ψ and the e^- beam. Following the steps elaborated in [24], the differential rate for polarized $J/\psi + \eta_{c2}$ production in e^+e^- annihilation can be expressed as

$$\frac{d\sigma[e^+e^- \to J/\psi(\lambda_1)+\eta_{c2}(\lambda_2)]}{d\cos\theta} = \frac{\alpha}{8s^2}\left(\frac{|\mathbf{P}|}{\sqrt{s}}\right)|\mathcal{A}_{\lambda_1,\lambda_2}|^2 \times \begin{cases} \frac{1+\cos^2\theta}{2} & (\lambda_1-\lambda_2=\pm 1) \\ \sin^2\theta & (\lambda_1-\lambda_2=0), \end{cases} \tag{2}$$

where $\mathcal{A}_{\lambda_1,\lambda_2}$ is the helicity amplitude associated with the virtual photon decay into $J/\psi + \eta_{c2}$ carrying the helicity component (λ_1, λ_2).

Parity invariance can be invoked to reduce the number of independent helicity amplitudes,

$$\mathcal{A}_{\lambda_1,\lambda_2} = -\mathcal{A}_{-\lambda_1,-\lambda_2}; \tag{3}$$

hence, the two helicity amplitudes related by flipping the helicities of two chamonia bear the equal magnitude. An immediate consequence of (3) is that the virtual photon decay into the longitudinally polarized J/ψ and η_{c2} is strictly forbidden by parity invariance.

Integrating (2) over the polar angle θ and including all the allowed helicity states, it is then straightforward to obtain the unpolarized cross section,

$$\sigma[e^+e^- \to J/\psi + \eta_{c2}] = \frac{\alpha\sqrt{1-4r}}{12s^2}(2|\mathcal{A}_{0,1}|^2 + 2|\mathcal{A}_{1,0}|^2 + 2|\mathcal{A}_{1,1}|^2 + 2|\mathcal{A}_{1,2}|^2). \tag{4}$$

In conformity with the constraint $|\lambda_1 - \lambda_2| \le 1$, as demanded by angular momentum conservation, there are totally 4 independent helicity amplitudes for $\gamma^* \to J/\psi + \eta_{c2}$ (Recall that $\mathcal{A}_{0,0} = 0$ owing to parity invariance). In Eq. (4), we have also retained a factor of 2 explicitly to account for the contributions from those helicity-flipped states. We have also adopted the approximation $\frac{2|\mathbf{P}|}{\sqrt{s}} \approx \sqrt{1-4r}$ by assuming $M_{J/\psi} \approx M_{\eta_{c2}} \approx 2m_c$.

In the NRQCD factorization framework, the product of two nonperturbative factors, i.e., the (second derivative of) wave functions at the origin for the charmonia J/ψ, and η_{c2} [$R_{J/\psi}(0)$, and $R''_{\eta_{c2}}(0)$] ubiquitously enter every helicity amplitude, thereby it appears convenient to define a *reduced* dimensionless helicity amplitude, from which these nonperturbative factors are pulled out. We introduce the reduced helicity amplitude, a_{λ_1,λ_2}, which is related to the standard helicity amplitude $\mathcal{A}_{\lambda_1,\lambda_2}$ as follows:

$$\mathcal{A}_{\lambda_1,\lambda_2} = \frac{2^8\sqrt{5}e_c e\alpha_s R_{J/\psi}(0)R''_{\eta_{c2}}(0)}{3sm_c^2} r^{\frac{1}{2}(|\lambda_1+\lambda_2|-1)} a_{\lambda_1,\lambda_2}(r), \tag{5}$$

where $e_c e = \frac{2}{3}e$ is the electric charge of the charm quark, $r \equiv 4m_c^2/s$ signifies a dimensionless mass ratio. To make the HSR manifest, we have explicitly stripped off a factor $r^{\frac{1}{2}(|\lambda_1+\lambda_2|-1)}$ in (5), so that the dimensionless helicity amplitude a_{λ_1,λ_2} is expected to scale as $\mathcal{O}(r^0)$.

Plugging (5) back into (4), we obtain the NRQCD predictions to the polarized production rate for the $J/\psi(\lambda_1) + \eta_{c2}(\lambda_2)$ state:

$$\sigma[e^+e^- \to J/\psi(\lambda_1)+\eta_{c2}(\lambda_2)] = \frac{5\times 2^{16}\pi e_c^2\alpha^2\alpha_s^2}{27s^4m_c^4} R^2_{J/\psi}(0)R''^2_{\eta_{c2}}(0) r^{|\lambda_1+\lambda_2|-1}(1-4r)^{\frac{1}{2}}|a_{\lambda_1,\lambda_2}|^2. \tag{6}$$

III. LO PREDICTIONS FOR THE HELICITY AMPLITUDES

The reduced helicity amplitude a_{λ_1,λ_2} can be viewed as the NRQCD short-distance coefficient, which encodes the contribution solely stemming from the momentum region between m_c and $\sqrt{s}$, so can be computed reliably in perturbation theory. It is convenient to parametrize it as

$$a_{\lambda_1,\lambda_2} = a^{(0)}_{\lambda_1,\lambda_2} + \frac{\alpha_s}{\pi} a^{(1)}_{\lambda_1,\lambda_2}. \tag{7}$$

Our central task in this work is to decipher the $\mathcal{O}(\alpha_s)$ correction to the reduced amplitude, $a^{(1)}_{\lambda_1,\lambda_2}$.

First, we recapitulate the LO calculation. To proceed, it most convenient to consider the quark amplitude $\gamma^* \to c\bar{c}({}^3S_1^{(1)}) + c\bar{c}({}^1D_2^{(1)})$ using the covariant projection technique [10,34]. At LO in α_s, there are only four Feynman diagrams that contribute, one of which is depicted in Fig. 1(a) (For simplicity, we have neglected the QED fragmentation diagrams, whose effect appears to be modest).

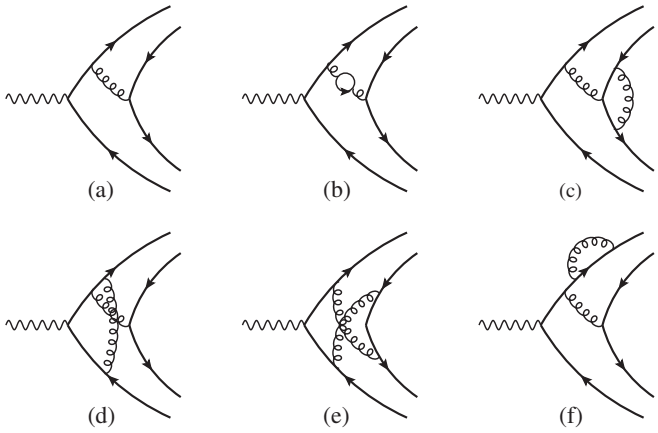

FIG. 1. One sample LO diagram and five sample NLO diagrams that contribute to $\gamma^* \to J/\psi + \eta_{c2}$.

It is straightforward to project out four corresponding helicity amplitudes from the decay amplitude for $\gamma^* \to J/\psi + \eta_{c2}$. One then follows Eq. (5) to read off each of the LO reduced helicity amplitudes:

$$a^{(0)}_{\lambda_1,\lambda_2} = \begin{cases} \pm(1-4r)^{\frac{3}{2}} & (\lambda_1,\lambda_2) = (\pm 1, 0) \\ 0 & (\lambda_1,\lambda_2) = \text{others}. \end{cases} \tag{8}$$

For some accidental reason, only the $J/\psi(\pm 1) + \eta_{c2}(0)$ channel has the nonvanishing cross section at LO in α_s. Substituting (8) into (6), we find agreement with the QCD part of the LO prediction for the unpolarized cross section first given in Ref. [10].

IV. NLO PERTURBATIVE CORRECTIONS TO THE HELICITY AMPLITUDES

We start this section by first sketching some technical issues about the NLO perturbative calculations, followed by presenting the asymptotic expressions of the $\mathcal{O}(\alpha_s)$ corrections to all the reduced helicity amplitudes.

A. Outline of the calculation

At NLO in α_s, there are 20 two-point, 20 three-point, 18 four-point, and 6 five-point one-loop diagrams for the process $\gamma^* \to c\bar{c}({}^3S_1^{(1)}) + c\bar{c}({}^1D_2^{(1)})$, some of which have been illustrated in Fig. 1. The calculation is quite similar to our preceding works on double charmonium exclusive production, i.e., $e^+e^- \to J/\psi + \chi_{c0,1,2}$ [24] and the $e^+e^- \to J/\psi + \eta_c$ [21], so here we will only present a very brief description.

We adopt dimensional regularization to regularize both UV and IR singularities. We follow the 't Hooft-Veltman prescription for γ_5, as detailed in Ref. [35]. In projecting out the D-wave orbital angular momentum state, one needs expand the relative quark momentum q to the quadratic order. Our strategy is to follow the method of region [36] via directly deducing the NRQCD short-distance coefficients, rather than resorting to the much more expensive matching calculation, through making the expansion in q before carrying out the loop integration.

The only nontrivial technical problem is that one may encounter some unusual one-loop integrals which generally contain the propagators of cubic power, as a consequence of taking the derivative over q twice. The MATHEMATICA package FIRE [37] and the code APART [38] are utilized to reduce these unconventional higher-point one-loop tensor integrals into a set of masters integrals. With the aid of the integration-by-part algorithm and partial fractioning technique, it turns out that all the encountered master integrals are nothing but the standard 2-point and 3-point one-loop scalar integrals, whose analytic expressions have already been tabulated in Ref. [17].

When adding the contributions of all the diagrams, and after renormalizing the charm quark mass and the QCD coupling constant, we finally end up with both UV and IR finite NLO expressions for the decay amplitude $\gamma^* \to c\bar{c}({}^3S_1^{(1)}) + c\bar{c}({}^1D_2^{(1)})$. Since everything becomes finite, we can safely return to the four spacetime dimensions and readily project out all the required helicity amplitudes.

In Ref. [39], an all-order-in-α_s proof for exclusive quarkonium production has been outlined in the NRQCD factorization context. It argues that at lowest order in v and to all orders in α_s, NRQCD factorization holds for the exclusive production of a S-wave quarkonium plus any higher-orbital-angular-momentum quarkonium in e^+e^- annihilation. Our explicit calculation confirms that the NRQCD short-distance coefficients affiliated with S-wave plus D-wave charmonia production are indeed IR finite at NLO in α_s, which is compatible with what is asserted in [39].

B. Analytic expressions of NLO helicity amplitudes

The $a^{(1)}_{\lambda_1,\lambda_2}$ are complex-valued, whose analytic expressions are in general quite lengthy. Rather than reproducing their cumbersome-looking expressions here, we are content with presenting their numerical values over a wide range of r, as shown in Fig. 2.

As a matter of fact, it seems much more illuminating to know the asymptotic behaviors of the helicity amplitudes in the limit $\sqrt{s} \gg m_c$. At NLO in α_s, one anticipates to see the logarithmic scaling violation to the naive power-law HSR as indicated in (1). Furthermore, conducting the asymptotic expansion in NRQCD short-distance coefficients is theoretically appealing, since it is equivalent to disentangling the contributions occurring at the "hard" scale (virtuality $\sim s$) from the "lower-energy" collinear/soft sectors (virtuality $\sim m_c^2$), by which one can intimately link the NRQCD factorization approach and the light-cone approach [40–44]. Such an asymptotic expansion on the NRQCD hard coefficients has been carried out for a number of exclusive double-quarkonium production processes, either in e^+e^- annihilation [21,24,44], or from bottomonium decay [44–47], and some general pattern about logarithmic scaling violation has been recognized [24,44].

According to the definition in (6), we find the asymptotic expressions of four reduced NLO helicity amplitudes for $\gamma^* \to J/\psi + \eta_{c2}$ to be

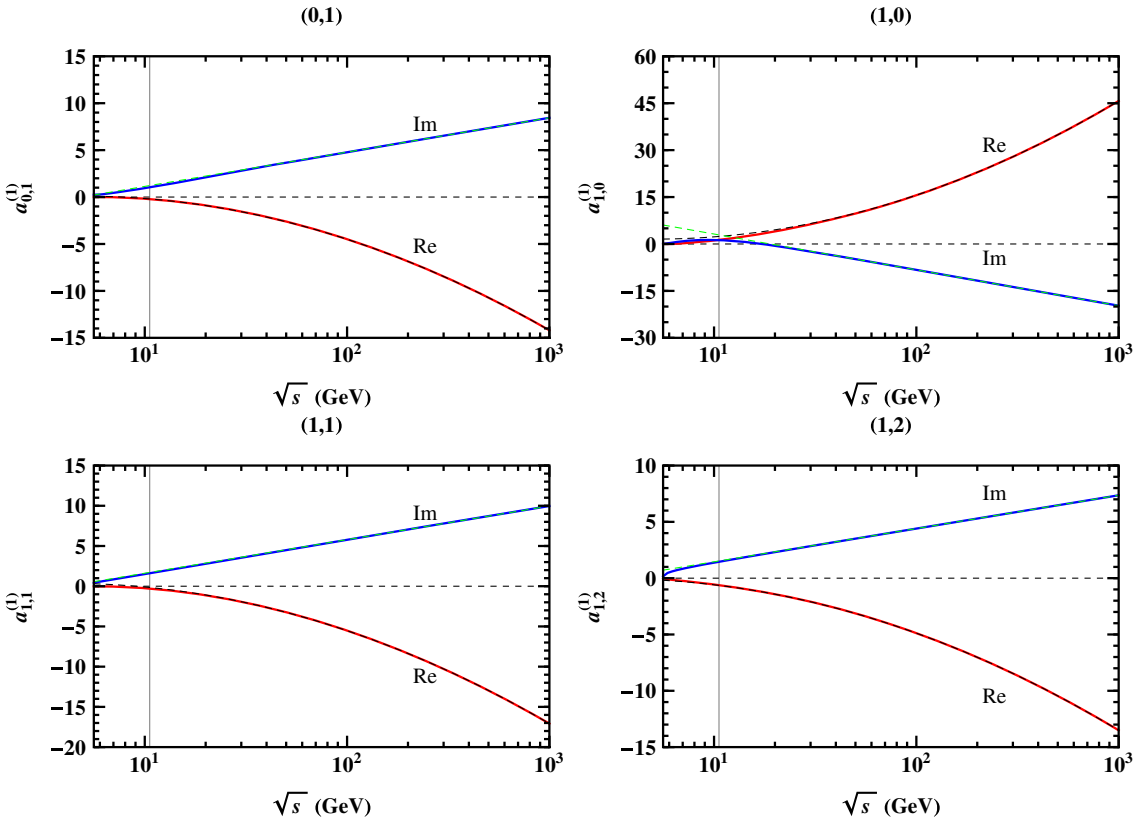

FIG. 2. Variation of the $\mathcal{O}(\alpha_s)$ reduced helicity amplitudes $a^{(1)}_{\lambda_1,\lambda_2}$ with $\sqrt{s}$. We take $\mu = \frac{\sqrt{s}}{2}$ and $m_c = 1.4$ GeV. The solid curves correspond to the exact NLO results, and the dashed curves represent the asymptotic ones as given in (9). The vertical mark is placed at the B factory energy $\sqrt{s} = 10.58$ GeV.

$$a^{(1)}_{0,1}\Big|_{\rm asym} = -\frac{\sqrt{3}}{96}\left\{7\ln^2 r - 2(22-43\ln 2)\ln r - \frac{286}{3} - 12\pi^2 + \frac{1024}{3}\ln 2 - 41\ln^2 2 + 2i\pi(7\ln r - 22 + 43\ln 2)\right\}, \quad (9a)$$

$$a^{(1)}_{1,0}\Big|_{\rm asym} = \frac{1}{48}\left\{19\ln^2 r + 19(1+2\ln 2)\ln r + 12\beta_0\left(\ln\frac{4\mu^2}{s} + \frac{8}{3}\right) - \frac{478}{3} + \frac{244}{3}\ln 2 - 129\ln^2 2 + i\pi(38\ln r + 12\beta_0 + 19 + 38\ln 2)\right\}, \quad (9b)$$

$$a^{(1)}_{1,1}\Big|_{\rm asym} = -\frac{\sqrt{3}}{24}\left\{2\ln^2 r + (19-23\ln 2)\ln r - \frac{16}{3} + \frac{9\pi^2}{2} - \frac{143}{3}\ln 2 - \frac{41}{2}\ln^2 2 + i\pi(4\ln r + 19 - 23\ln 2)\right\}, \quad (9c)$$

$$a^{(1)}_{1,2}\Big|_{\rm asym} = -\frac{\sqrt{6}}{24}\left\{\ln^2 r - 7(2-3\ln 2)\ln r - \frac{15}{2} - \frac{19\pi^2}{6} + 51\ln 2 - \frac{17}{2}\ln^2 2 + i\pi(2\ln r - 14 + 21\ln 2)\right\}, \quad (9d)$$

where μ is the renormalization scale, and $\beta_0 = \frac{11}{3}C_A - \frac{2}{3}n_f$ is the one-loop coefficient of the QCD β function, and $n_f = 4$ denotes the number of active quark flavors. In contrast with (8), all four reduced helicity amplitudes receive nonvanishing $\mathcal{O}(\alpha_s)$ corrections.

Note that the $\beta_0 \ln(4\mu^2/s)$ term only resides in the $(\pm 1, 0)$ channel, since this is the only channel that has a nonvanishing tree-level amplitude. For the sake of comparison, all these asymptotic results of the reduced helicity amplitudes are also shown in Fig. 2, in juxtapose with the corresponding exact NLO results. These asymptotic results appear to converge with the exact ones decently well even at relatively lower $\sqrt{s}$, say, at B factory energy.

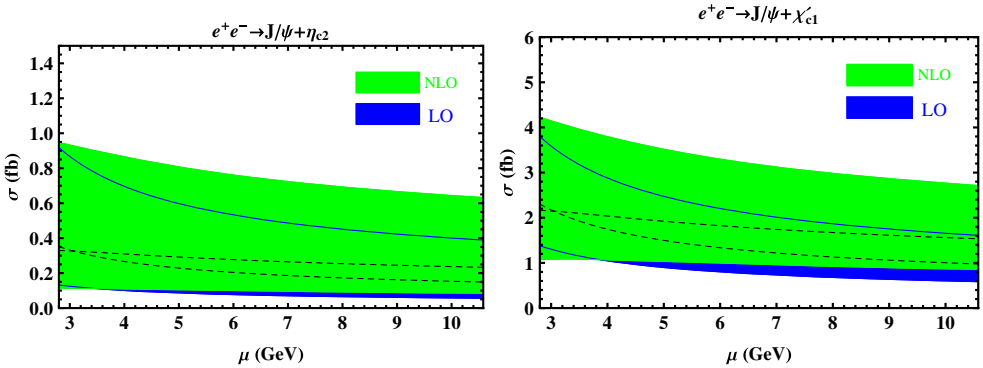

FIG. 3. The renormalization scale dependence of the LO and NLO cross sections for $e^+e^- \to J/\psi + \eta_{c2}$ (left panel) and $e^+e^- \to J/\psi + \chi'_{c1}$ (right panel) at $\sqrt{s} = 10.58$ GeV. The band is obtained by varying the charm quark mass in the range $m_c = 1.4 \pm 0.2$ GeV.

From Eq. (9), one sees that the leading scaling violation is due to the double logarithm $\ln^2 r$. This constitutes another example to further corroborate the earlier conjecture: the occurrence of $\ln^2 r$ in the one-loop NRQCD short-distance coefficients is always affiliated with the helicity-suppressed channels in exclusive double charmonium production processes [24,44].

V. PHENOMENOLOGY

Aside from a comprehensive analysis on the process $e^+e^- \to J/\psi + \eta_{c2}$ at the B factory, in this section we also target at a detailed investigation on the process $e^+e^- \to J/\psi + \chi'_{c1}$, where the essential elements have already been set up in [24]. This study is largely motivated by the recent concern about the nature of the $X(3872)$ meson, whether its quantum number is 1^{++} or 2^{-+}. The canonical charmonium options for the $X(3872)$ are the χ'_{c1} and η_{c2}, respectively. With this consideration in mind, our study may provide some useful guidance on unveiling the quantum number of the $X(3872)$ through the dedicated double-charmonium experiment at the future B factory.

Before making concrete predictions to the production rates for $e^+e^- \to J/\psi + \eta_{c2}$, we first address a subtlety about utilizing (6). For the $J/\psi(\pm 1) + \eta_{c2}(0)$ helicity state, the canonic way of identifying the $\mathcal{O}(\alpha_s)$ correction is by replacing $|a_{\pm 1,0}|^2$ with $2\frac{\alpha_s}{\pi}\Re[a^{(0)}_{\pm 1,0}a^{(1)}_{\pm 1,0}]$. Because of the null tree-level amplitudes for the remaining helicity configurations, the $\mathcal{O}(\alpha_s)$ correction to the total cross section is solely from the $(\pm 1, 0)$ channels. On the other hand, the polarized cross section for each helicity state is also a physical observable by itself. Since the nonvanishing amplitudes are first generated at $\mathcal{O}(\alpha_s)$ for the remaining helicity states, it is thereby also sensible to interpret $|a_{\lambda_1,\lambda_2}|^2 = (\frac{\alpha_s}{\pi})^2|a^{(1)}_{\lambda_1,\lambda_2}|^2$ for $(\lambda_1, \lambda_2) \neq (\pm 1, 0)$. Though formally of order α_s^2, these new pieces do constitute the leading contributions to the respective polarized cross sections, thereby still being consistent.[2] We will follow this viewpoint in presenting our NLO predictions.

In the numerical analysis, we take $\sqrt{s} = 10.58$ GeV, and the charm quark pole mass $m_c = 1.4 \pm 0.2$ GeV. The fine structure constant is chosen as $\alpha(\sqrt{s}) = 1/130.9$ [19]. The running QCD strong coupling constant is evaluated by using the two-loop formula with $\Lambda^{(4)}_{\overline{\rm MS}} = 0.338$ GeV [16,17]. The nonpertubative input parameters, i.e., (the derivatives of) the wave function at the origin for $J/\psi, \chi'_{c1}$, and η_{c2}, also suffer from a large amount of uncertainty. Their values have been compiled in Ref. [48], which were deduced from several different potential models. We choose to use those given by the Buchmüller-Tye potential model [49]: $|R_{J/\psi}(0)|^2 = 0.81\ \text{GeV}^3$, $|R'_{\chi'_{c1}}(0)|^2 = 0.102\ \text{GeV}^5$, and $|R''_{\eta_{c2}}(0)|^2 = 0.015\ \text{GeV}^7$.

Another important source of uncertainty for the NLO predictions stems from the scale affiliated with the strong coupling constant. As is well known, the scale ambiguity is a typical nuisance of NRQCD factorization approach, reflecting the fact that two disparate hard scales, $\sqrt{s}$ and m_c, are entangled together in NRQCD short-distance coefficients. In fact, the lesson gained from the light-cone approach strongly suggests that it is rather implausible to set the scales entering all α_s in NLO short-distance coefficient to be unanimously around $\sqrt{s}$ [44]. Although we are unable to circumvent the scale ambiguity problem in the confine of NRQCD approach, we may allow the μ to float in the range between $2m_c$ and $\sqrt{s}$, hoping that the most trustworthy prediction may interpolate in between.

In Fig. 3, we show the total cross sections both for $e^+e^- \to J/\psi + \eta_{c2}$ and $e^+e^- \to J/\psi + \chi'_{c1}$ as a function of μ, which also take into account the error due to the

[2]The uncalculated order-v^2 corrections to $e^+e^- \to J/\psi + \eta_{c2}$ generally also lead to nonvanishing amplitudes for those helicity states other than $(\pm 1, 0)$, which are potentially as important as the $\mathcal{O}(\alpha_s)$ corrections. For the leading contributions to the corresponding polarized cross sections, one needs also include the interference effect between the radiative and relativistic corrections.

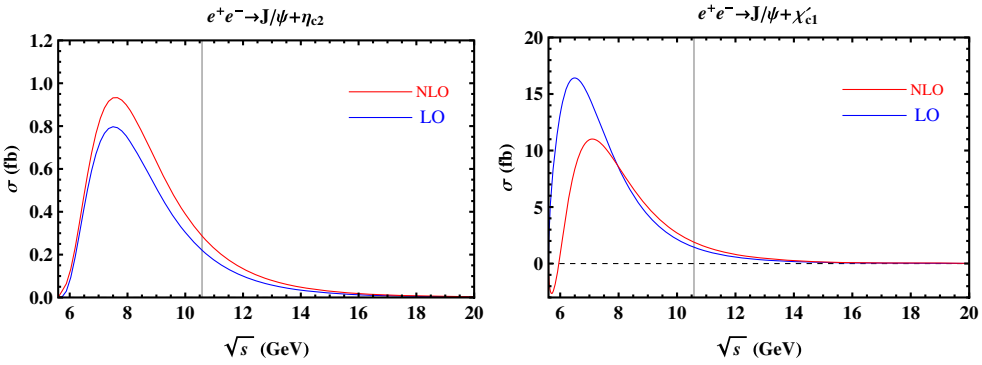

FIG. 4. Variation of the LO and NLO cross sections for $e^+e^- \to J/\psi + \eta_{c2}$ (left panel) and $e^+e^- \to J/\psi + \chi'_{c1}$ (right panel) with $\sqrt{s}$. m_c is fixed as 1.4 GeV and the renormalization scale is taken as $\mu = \frac{\sqrt{s}}{2}$.

uncertainty of m_c. One sees clearly that, after incorporating the NLO perturbative correction, the scale dependence of the cross section has been reduced. In Fig. 4, we also plot the LO and NLO total cross sections for $e^+e^- \to J/\psi + \eta_{c2}$ as a function of $\sqrt{s}$. Since the leading-twist (0, 0) channel is absent in both of the processes, the cross sections drop very rapidly ($\propto 1/s^4$) as $\sqrt{s}$ increases.

In Tables I and II, we also list the predictions for the polarized cross sections from each individual helicity channel as well as the total cross sections for $e^+e^- \to J/\psi + \eta_{c2}$ and $e^+e^- \to J/\psi + \chi'_{c1}$, with m_c fixed at 1.4 GeV but with the renormalization scale chosen at three different points. The impact of the $\mathcal{O}(\alpha_s)$ corrections to the total cross sections is surprisingly alike for both double-charmonium production processes: incorporating the NLO pertubative correction decreases the LO cross sections by about 6% for $\mu = 2m_c$, or increases the LO result by roughly 30% for $\mu = \sqrt{s}/2$, or enhances the LO result by about 60% for $\mu = \sqrt{s}$. Hence, the relative importance of the $\mathcal{O}(\alpha_s)$ correction increases as μ increases. Taking the medium value $\mu = \sqrt{s}/2$, our NLO predictions for the cross sections of $e^+e^- \to J/\psi + \eta_{c2}$ and $e^+e^- \to J/\psi + \chi'_{c1}$ at $\sqrt{s} = 10.58$ GeV reach about 0.3 fb and 1.9 fb, respectively. The production rate of the latter process is about 6 times more copious than that of the former.

Inspecting Tables I and II, one observes an interesting hierarchy of the polarized cross sections for the above processes. The overwhelming contribution for the $J/\psi + \eta_{c2}$ production comes solely from the $(\pm 1, 0)$ state, with J/ψ transversely polarized, while the dominant

TABLE I. Polarized and total cross sections (in unit of fb) for $e^+e^- \to J/\psi + \eta_{c2}$. We have taken $m_c = 1.4$ GeV. In the rightmost column, we also give the K factor for the unpolarized cross sections.

		$\sigma_{(1,0)}$	$\sigma_{(0,1)}$	$\sigma_{(1,1)}$	$\sigma_{(1,2)}$	$\sigma_{\rm tot}$	K
$\mu = 2m_c$	LO	0.18	…	…	…	0.35	0.94
	NLO	0.17	3.4×10^{-3}	5.5×10^{-4}	3.7×10^{-5}	0.33	
$\mu = \frac{\sqrt{s}}{2}$	LO	0.11	…	…	…	0.22	1.30
	NLO	0.14	1.5×10^{-3}	2.4×10^{-4}	1.6×10^{-5}	0.29	
$\mu = \sqrt{s}$	LO	7.4×10^{-2}	…	…	…	0.15	1.57
	NLO	0.12	6.8×10^{-4}	1.1×10^{-4}	7.5×10^{-6}	0.23	

TABLE II. Polarized and total cross sections (in unit of fb) for $e^+e^- \to J/\psi + \chi'_{c1}$. We have taken $m_c = 1.4$ GeV. In the rightmost column, we also list the K factor for the unpolarized cross sections.

		$\sigma_{(1,0)}$	$\sigma_{(0,1)}$	$\sigma_{(1,1)}$	$\sigma_{\rm tot}$	K
$\mu = 2m_c$	LO	2.3×10^{-3}	1.07	0.082	2.30	0.94
	NLO	−0.026	1.08	0.033	2.16	
$\mu = \frac{\sqrt{s}}{2}$	LO	1.4×10^{-3}	0.67	0.051	1.44	1.31
	NLO	−0.012	0.91	0.045	1.89	
$\mu = \sqrt{s}$	LO	9.7×10^{-4}	0.45	0.035	0.98	1.57
	NLO	−0.0063	0.73	0.042	1.53	

helicity channel for producing $J/\psi+\chi'_{c1}$ is instead the $(0,\pm1)$ state, with J/ψ longitudinally polarized. This characteristic of J/ψ polarization may serve as a benchmark for the future double-charmonium production experiment to unveil the nature of the $X(3872)$, provided that the prospective Super B factory can observe sufficient number of $X(3872)$ events recoiling against J/ψ. From Table II, one also notes that the NLO corrections to the cross sections in the (1,0) channel become negative. This signals substantial negative $\mathcal{O}(\alpha_s)$ corrections associated with this channel, which also implies that even higher-order radiative corrections might also be important.

We can ascertain the observation potential of these two exclusive double charmonium production processes. Thus far, BELLE experiment has accumulated about 1000 fb^{-1} data. Taking $\sigma[e^+e^-\to J/\psi+\eta_{c2}]\approx 0.23$–$0.33$ and $\sigma[e^+e^-\to J/\psi+\chi'_{c1}]\approx 1.53$–$2.16$ fb from Tables I and II, we estimate that roughly 230–330 $J/\psi+\eta_{c2}$ events, and 1500–2200 $J/\psi+\chi'_{c1}$ events have been produced at BELLE at around $\sqrt{s}=10.58$ GeV.

Since neither of the masses and decay patterns of η_{c2} and χ'_{c1} is known, it seems experimentally impossible to simultaneously reconstruct the J/ψ and the $\eta_{c2}(\chi'_{c1})$ signals. The viable experimental way is to only reconstruct the $J/\psi\to l^+l^-$ event, and fit the recoil mass spectrum against the J/ψ to estimate the number of $\eta_{c2}(\chi'_{c1})$ peak events. This method does not depend on the concrete decay modes of $\eta_{c2}(\chi'_{c1})$, and is particularly suitable for the limited statistics of signal events like in our case. In fact, this method has already been used routinely by the BELLE Collaboration to search for the double charmonium production processes $e^+e^-\to J/\psi+C$-even charmonium.

In fitting the recoil mass spectrum, the net detection efficiency for $e^+e^-\to J/\psi+\eta_{c2}(\chi'_{c1})$ may reach around 4% (Similar for η_{c2} and χ'_{c1}, with the reconstruction efficiency for $J/\psi\to l^+l^-$ included [50]). As a very crude estimate, the number of observed $e^+e^-\to J/\psi+\eta_{c2}(\chi'_{c1})$ events are expected to reach $(230-330)\times 4\%=9-13$, and $(1500-2200)\times 4\%=60-90$, respectively. Since only the J/ψ is reconstructed, the background level can be a little higher. With only around 9–13 observed $J/\psi+\eta_{c2}$ events, it appears difficult to observe a significant signal with current 1 ab^{-1} BELLE data. If χ'_{c1} is indeed the $X(3872)$ meson, thanks to the very narrow width of the $X(3872)$, it seems possible to observe the 60–90 $J/\psi+\chi'_{c1}$ signal events with the current BELLE full data sample, which may provide a strong incentive for updating their earlier $e^+e^-\to J/\psi+$ charmonium analysis with only 673 fb^{-1} data [5,51]. This study may hopefully help one to better understand the mechanism about the $X(3872)$ production. On the other hand, in case that χ'_{c1} is not $X(3872)$ and its width is no longer narrow, it may be difficult to observe a significant signal at the moment.

In any event, a much larger data samples seem to be called for to arrive at some definite conclusion. In the prospective Super B factory, which may reach an integrated luminosity of 50 ab^{-1} by 2022, it seems feasible that the processes $e^+e^-\to J/\psi+\eta_{c2}(\chi'_{c1})$ will eventually be observed, and the quantum number of $X(3872)$ also hopefully be nailed down.

VI. SUMMARY

In this work, we have calculated the complete NLO perturbative corrections to $e^+e^-\to J/\psi+\eta_{c2}$ within the NRQCD factorization framework, and found that the $\mathcal{O}(\alpha_s)$ correction can be sizable for a larger value of the renormalization scale. Our calculation indicates that the dominate contribution to the total cross section comes from the helicity states $(\pm1,0)$.

We have also carried out a comparative study for $e^+e^-\to J/\psi+\eta_{c2}$ and $e^+e^-\to J/\psi+\chi'_{c1}$ at B factory energy, with the specific motivation that these double charmonium production processes may provide useful means to unveil the quantum number of the $X(3872)$ meson in the future B factories. It turns out that the production rate of the latter process is about 6–7 times greater than the former; therefore, it is possible to observe the $J/\psi+\chi'_{c1}$ signals based on the current 1 ab^{-1} BELLE data sample, if the χ'_{c1} is indeed the very narrow $X(3872)$ particle. The dominantly transverse polarization of the J/ψ is also a useful indicator for identifying the $X(3872)$ with χ'_{c1}.

A necessary extension of our current work is to further incorporate the leading relativistic correction to the above double-charmonium production processes, whose effects might be as important as the radiative corrections. The study along this direction is of some theoretical interest, especially regarding that, until today the $\mathcal{O}(v^2)$ calculation hardly exists for the production processes involving the P, D-wave quarkonium.

It has been recently realized that the $\mathcal{O}(\alpha_s)$ NRQCD short-distance coefficients for the helicity-suppressed double charmonium-production processes are often plagued with the double logarithm of form $\ln^2(s/m_c^2)$ [44]. This symptom is likely intertwined with some long-standing failure of applying the light-cone approach to the "higher-twist" hard exclusive reactions beyond tree level, such as $\gamma^*\rho\pi$ transition form factor [8]. To expedite a better understanding and controlling of these double logarithms, we have scrutinized all the NLO diagrams for the various exclusive double-charmonium processes that have been studied so far, e.g., $e^+e^-\to J/\psi+\eta_{c2}(\eta_c,\chi_{c0,1,2})$, and singled out those that contain double logarithms, and enumerate their coefficients for each individual helicity states. No simple and general pattern has been recognized yet.

ACKNOWLEDGMENTS

We are grateful to Wen-Long Sang for an independent check of some part of our calculations. We also thank Cheng-

Ping Shen for helpful discussions on experimental issues. The work of F. F. is supported by the National Natural Science Foundation of China under Grant No. 11505285, and by the Yue Qi Young Scholar Project in CUMTB. The work of Y. J. is supported in part by the National Natural Science Foundation of China under Grants No. 11475188, No. 11261130311, No. 11621131001 (CRC110 by DGF and NSFC), by the IHEP Innovation Grant under Contract No. Y4545170Y2, and by the State Key Lab for Electronics and Particle Detectors. The Feynman diagrams in this paper are prepared using JaxoDraw [52,53].

APPENDIX: ANATOMY OF THE NLO DIAGRAMS CONTAINING DOUBLE LOGARITHMS IN VARIOUS DOUBLE-CHARMONIUM PRODUCTION PROCESSES

Although the NRQCD factorization approach and the light-cone approach are based on two completely different expansion strategies, they can be intimately linked for the exclusive double charmonium production processes in the limit $s \gg m_c^2$. As exemplified by an anatomy of the $\mathcal{O}(\alpha_s)$ correction to the B_c electromagnetic form factor [44], the light-cone approach can be efficiently utilized to reproduce the asymptotic behavior of the $\mathcal{O}(\alpha_s)$ NRQCD short-distance coefficient through the idea of refactorization [41–43].

It is worth emphasizing one important limitation of the refactorization procedure. So far it can only be successfully applied to the "leading-twist" reactions involving quarkonium, that is, with the HSR-favored helicity configurations. A general characteristic about this class of processes is that, at the NLO in α_s, only the single collinear logarithm of $\ln\frac{s}{m_c^2}$ arises in the NRQCD short-distance coefficient, which can be resummed to all orders in α_s with the aid of the Brodsky-Lepage evolution equation. This feature has been explicitly verified in several examples, e.g., $\gamma^* \to \eta_c + \gamma$ [40,43,54], $\gamma^* + B_c \to B_c$ [43], $\gamma^* \to J/\psi(0) + \chi_{c0,2}(0)$ [24].

However, the majority of phenomenologically relevant double-charmonia production processes are of "higher-twist" nature, exemplified by $\gamma^* \to J/\psi + \eta_{c2}(\eta_c, \chi_{c0,1,2})$, for which some of or all possible helicity channels are of the HSR-suppressed type. Until today, it is still not clear how to consistently compute the NLO radiative correction to this type of processes in the light-cone framework, due to some long-standing problem such as the inevitable emergence of the end-point singularity. By contrast, NRQCD factorization approach, which is based on the velocity expansion rather than the twist expansion, serves as the *only* viable tool to investigate the $\mathcal{O}(\alpha_s)$ corrections to this kind of helicity-suppressed hard exclusive reactions.

An abnormal feature about the $\mathcal{O}(\alpha_s)$ NRQCD short-distance coefficients for the helicity-suppressed double charmonium production processes seems to be the frequent emergence of the double logarithm $\ln^2(s/m_c^2)$, which seems to seriously deteriorate the convergence of the perturbative expansion in NRQCD factorization.[3] This double logarithm appears to result from the overlap between the "collinear" and "soft" regions in the NRQCD short-distance coefficient and seems deeply related to the aforementioned end-point singularity problem. Although it is feasible to reproduce the closed form of the double logarithms for each concrete process, the lack of a thorough understanding of their behavior in higher order in α_s prevents one from systematically controlling them, i.e., resumming them to all orders in α_s.

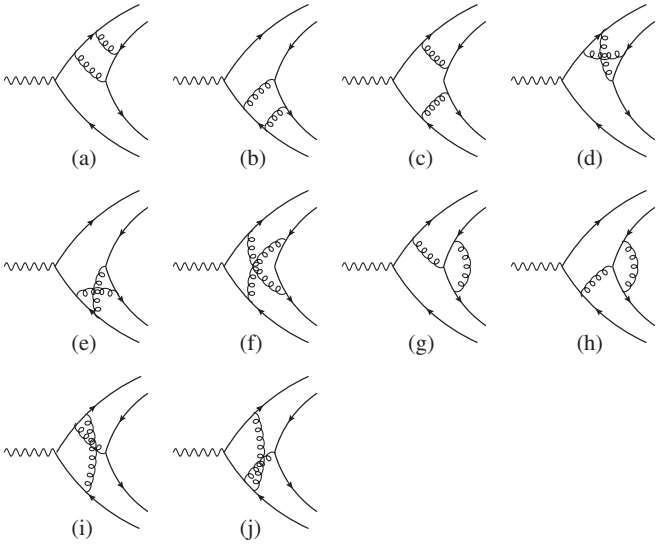

FIG. 5. The NLO diagrams that contain the double logarithm $\ln^2(s/m_c^2)$ (in Feynman gauge) for the process $\gamma^* \to J/\psi + \eta_{c2}(\eta_c, \chi_{c0,1,2})$. The respective charge-conjugated diagrams have been suppressed.

A useful starting point is to anatomize all the double logarithms of form $\ln^2(s/m_c^2)$ from the existing NLO calculations for the various exclusive double charmonium processes. For this purpose, we examine all the NLO Feynman diagrams for the processes $e^+e^- \to J/\psi + \eta_{c2}(\eta_c, \chi_{c0,1,2})$, sort out those that contain the double logarithm, and enumerate their coefficients.

A careful examination reveals that (almost) all the relevant NLO diagrams that contribute the double logarithm $\ln^2(s/m_c^2)$ (in Feynman gauge) for the above processes are included in Fig. 5, which was first identified in [44].

In Table III, we tabulate the double logarithms that come from each individual diagram in Fig. 5, with the color-structure specified, for the processes $e^+e^- \to J/\psi + \eta_{c2}(\eta_c)$.

[3]In fact, one will encounter the double logarithm even in the single-quarkonium exclusive production process such as $\gamma^* \to \eta_c + \gamma$, once the corresponding $\mathcal{O}(\alpha_s)$ NRQCD short-distance coefficient is expanded to NLO in m_c^2/s. This can be readily checked by using the analytic $\mathcal{O}(\alpha_s)$ short-distance coefficient given in [40,54].

TABLE III. The coefficients of the double logarithm associated with each diagram in Fig. 5 from the various helicity states (λ_1, λ_2) in the processes $\gamma^* \to J/\psi + \eta_{c2}(\eta_c)$. The two types of color factors are denoted by $C_1 = C_F^2$ and $C_2 = C_F(C_F - \frac{1}{2}C_A)$, where $C_F = \frac{4}{3}$ and $C_A = 3$.

Diagrams		*a)*	*b)*	*c)*	*d)*	*e)*	*f)*	*g)*	*h)*	*i)*	*j)*
Color Factor		C_1	C_1	C_1	C_2	C_2	C_2	C_2	C_2	C_2	C_2
η_{c2}	(1,0)	$\frac{3}{64}$	$\frac{9}{128}$	$\frac{3}{256}$	$\frac{9}{64}$	$\frac{3}{128}$	$\frac{21}{128}$	$-\frac{9}{128}$	$-\frac{3}{128}$	$-\frac{9}{128}$	$-\frac{3}{128}$
	(0,1)	…	$-\frac{3\sqrt{3}}{128}$	…	…	…	$-\frac{3\sqrt{3}}{128}$	…	…	…	…
	(1,1)	…	$-\frac{3\sqrt{3}}{256}$	$\frac{3\sqrt{3}}{256}$	…	…	…	…	…	…	…
	(1,2)	…	$-\frac{3\sqrt{6}}{256}$	…	…	…	…	…	…	…	…
η_c	(1,0)	$\frac{3}{64}$	$\frac{3}{32}$	$\frac{3}{128}$	$\frac{3}{32}$	$\frac{3}{64}$	$\frac{9}{64}$	$-\frac{3}{64}$	$-\frac{3}{64}$	$-\frac{3}{64}$	$-\frac{3}{64}$

TABLE IV. The coefficients of the double logarithm associated with each diagram in Fig. 5 from the various helicity states (λ_1, λ_2) in the process $\gamma^* \to J/\psi + \chi_{c0,1,2}$. The two types of color factors are represented by $C_1 = C_F^2$ and $C_2 = C_F(C_F - \frac{1}{2}C_A)$.

Diagrams		*a)*	*b)*	*c)*	*d)*	*e)*	*f)*	*g)*	*h)*	*i)*	*j)*
Color Factor		C_1	C_1	C_1	C_2	C_2	C_2	C_2	C_2	C_2	C_2
χ_{c0}	(1,0)	$\frac{7}{96}$	$\frac{1}{48}$	$\frac{1}{192}$	$\frac{1}{24}$	$\frac{7}{96}$	$\frac{11}{96}$	$-\frac{1}{48}$	$-\frac{7}{96}$	$-\frac{1}{48}$	$-\frac{7}{96}$
χ_{c1}	(1,0)	…	$-\frac{3}{32}$	$-\frac{3}{64}$	$-\frac{3}{16}$	$\frac{3}{32}$	$-\frac{3}{32}$	$\frac{3}{32}$	$-\frac{3}{32}$	$\frac{3}{32}$	$-\frac{3}{32}$
	(0,1)	$\frac{9}{128}$	$\frac{3}{64}$	$\frac{9}{256}$	$\frac{3}{128}$	$\frac{9}{128}$	$\frac{9}{64}$	$-\frac{3}{128}$	$-\frac{9}{128}$	$-\frac{3}{128}$	$-\frac{9}{128}$
	(1,1)	$\frac{27}{256}$	$\frac{3}{128}$	$-\frac{3}{256}$	$-\frac{3}{128}$	$\frac{15}{128}$	$\frac{3}{32}$	$\frac{3}{128}$	$-\frac{15}{128}$	$\frac{3}{128}$	$-\frac{15}{128}$
χ_{c2}	(0,1)	$\frac{3}{64}$	$\frac{3}{32}$	$\frac{3}{128}$	$\frac{3}{64}$	$\frac{3}{64}$	$\frac{3}{16}$	$-\frac{3}{64}$	$-\frac{3}{64}$	$-\frac{3}{64}$	$-\frac{3}{64}$
	(1,0)	$\frac{1}{32}$	$\frac{1}{16}$	$\frac{1}{64}$	$\frac{1}{8}$	$\frac{3}{32}$	$\frac{5}{32}$	$-\frac{1}{16}$	$-\frac{1}{32}$	$-\frac{1}{16}$	$-\frac{1}{32}$
	(1,1)	$\frac{9}{256}$	$\frac{9}{128}$	$-\frac{9}{256}$	$\frac{15}{128}$	$\frac{3}{128}$	$\frac{15}{64}$	$-\frac{9}{128}$	$-\frac{3}{128}$	$-\frac{9}{128}$	$-\frac{3}{128}$
	(1,2)	…	$\frac{3}{64}$	$\frac{3}{64}$	$\frac{3}{32}$	…	$\frac{9}{32}$	$-\frac{3}{32}$	…	$-\frac{3}{32}$	…

The reaction $e^+e^- \to J/\psi(\lambda_1) + \eta_c(\lambda_2)$ only possesses one independent helicity configuration $(\pm 1, 0)$. Each diagram contains a nonvanishing double logarithm. Summing up all their contributions, and multiply by 2 to account for the contribution from the charge-conjugated diagrams, we recover the net double logarithm in the NLO short-distance coefficient: $\frac{C^{(1)}}{C^{(0)}}|_{\rm asym} = \frac{13}{24}\ln^2\frac{s}{m_c^2}$, as given in Eq. (37) of Ref. [44].

All the four polarized production channels $e^+e^- \to J/\psi(\lambda_1) + \eta_{c2}(\lambda_2)$ are helicity-suppressed. Adding up the contributions from all the diagrams in Fig. 5, and multiplying by 2, we recover the net double logarithm in the NLO reduced helicity amplitudes $a^{(1)}_{\lambda_1,\lambda_2}|_{\rm asym}$, as given in Eqs. (9). Note that the double logarithms from the $(\pm 1, 0)$ channel has the similar diagram-by-diagram structure as its counterpart for $e^+e^- \to J/\psi + \eta_c$. Nevertheless, for the remaining three helicity channels, a great simplification arises that many of the diagrams in Fig. 5 do not contain double logarithm.

Next we examine the double logarithms that are affiliated with the polarized production processes $e^+e^- \to J/\psi(\lambda_1) + \chi_{cJ}(\lambda_2)$ $(J = 0,\ 1,\ 2)$. Excluding two helicity-conserved channels $\gamma^* \to J/\psi(0) + \chi_{c0,2}(0)$, Table IV lists the structure of double logarithms in the remaining eight helicity-suppressed channels. A noteworthy thing is that, for the helicity channel $(\pm 1, \pm 2)$ of $\gamma^* \to J/\psi + \chi_{c2}$, besides the diagrams shown in Fig. 5, one extra NLO diagram as shown in Fig. 6 also need be included. The color factor associated with the diagram in Fig. 6 is $\frac{1}{2}C_F$, and the corresponding coefficient is $-\frac{9}{16}$.

Adding up the contributions from all the diagrams in Fig. 5 for the reactions $e^+e^- \to J/\psi(\lambda_1) + \chi_{c0,1,2}(\lambda_2)$, together with that in Fig. 6 for the $(\pm 1, \pm 2)$ state, and multiplying the results by 2, we then reproduce the net

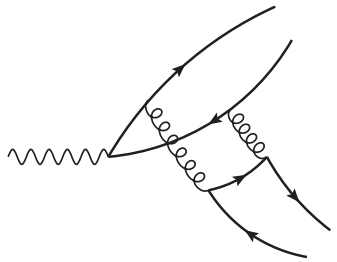

(k)

FIG. 6. The extra NLO diagram relative to Fig. 5 that also contributes the double logarithm $\ln^2(s/m_c^2)$ (in Feynman gauge) to the helicity channel $(\pm 1, \pm 2)$ for $\gamma^* \to J/\psi + \chi_{c2}$. The respective charge-conjugated diagram is not shown.

double logarithms in the NLO reduced helicity amplitudes, $K^J_{\lambda_1,\lambda_2}(r, \frac{\mu^2}{s})_{\rm asym}$ given in Eqs. (14) through (16) in Ref. [24].

An obvious observation from Tables III and IV is that the specific structures of the double logarithms are process-dependent. It seems that no simple, unified pattern can be readily recognized.

It is worth mentioning that the origin of the double logarithms for the $e^+e^- \to J/\psi + \eta_c$ has recently been clarified [55]. The authors distinguished two types of double logarithms which may arise in an individual NLO diagram, e.g., the Sudakov double logarithm and the *end-point logarithm* where a spectator quark line in loop diagram becomes soft. Upon summing all the NLO diagrams, it is found that the Sudakov double logarithms cancel, but the end-point logarithms remain [55].

It is also interesting to conduct an analogous anatomy, on a diagram-by-diagram basis, for the processes considered in this work, e.g., J/ψ associated production with a P, D-wave charmonium. Closely examining the collinear/soft momentum regions in the one-loop contributions to the NRQCD short-distance coefficients, one should be able to identify the origin of double logarithms. We believe that it is very likely that the pattern observed in Ref. [55] will reproduce in our processes; i.e., only the end-point double logarithms survive ultimately.

It is still an open challenge to thoroughly understand these apparently *nonuniversal* end-point double logarithms associated with the helicity-flipped double-charmonium production processes. The goal of resumming such double logarithms to all orders in α_s still looks rather remote. However, practically speaking, it may turn to be useful to first deduce the leading logarithms associated with the next-to-next-to-leading-order radiative corrections to NRQCD short-distance coefficients, which is possibly of quartic form $\ln^4 \frac{s}{m_c}$. This is undoubtedly a rather difficult task, but may still be approachable in view of recent technical advancement in higher-order perturbative calculation.

Finally, we would like to remark that the occurrence of double logarithms are not specific to the double-charmonium production, or helicity-flip process. For a simple example, consider the helicity-conserving single-charmonium production process, $e^+e^- \to \eta_c + \gamma$ [40,54]. In this case, the double logarithm also arises when the corresponding one-loop NRQCD short-distance coefficients is expanded to the next-to-leading power in m_c^2/s. Therefore, it seems more correct to state that double logarithms in exclusive charmonium production are always linked with the "higher-twist" contributions in the context of refactorizing the NRQCD short-distance coefficients [43].

[1] K. Abe *et al.* (Belle Collaboration), Phys. Rev. Lett. **89**, 142001 (2002).
[2] K. Abe *et al.* (Belle Collaboration), Phys. Rev. D **70**, 071102 (2004).
[3] B. Aubert *et al.* (*BABAR* Collaboration), Phys. Rev. D **72**, 031101 (2005).
[4] For a recent review, see N. Brambilla *et al.*, Eur. Phys. J. C **71**, 1534 (2011).
[5] K. Abe *et al.* (Belle Collaboration), Phys. Rev. Lett. **98**, 082001 (2007).
[6] P. Pakhlov *et al.* (Belle Collaboration), Phys. Rev. Lett. **100**, 202001 (2008).
[7] G. P. Lepage and S. J. Brodsky, Phys. Rev. D **22**, 2157 (1980).
[8] V. L. Chernyak and A. R. Zhitnitsky, Phys. Rep. **112**, 173 (1984).
[9] G. T. Bodwin, E. Braaten, and G. P. Lepage, Phys. Rev. D **51**, 1125 (1995); **55**, 5853(E) (1997).
[10] E. Braaten and J. Lee, Phys. Rev. D **67**, 054007 (2003).
[11] K. Y. Liu, Z. G. He, and K. T. Chao, Phys. Lett. B **557**, 45 (2003).
[12] K. Hagiwara, E. Kou, and C. F. Qiao, Phys. Lett. B **570**, 39 (2003).
[13] J. P. Ma and Z. G. Si, Phys. Rev. D **70**, 074007 (2004).
[14] A. E. Bondar and V. L. Chernyak, Phys. Lett. B **612**, 215 (2005).
[15] G. T. Bodwin, D. Kang, and J. Lee, Phys. Rev. D **74**, 114028 (2006).
[16] Y.-J. Zhang, Y.-J. Gao, and K.-T. Chao, Phys. Rev. Lett. **96**, 092001 (2006).
[17] B. Gong and J. X. Wang, Phys. Rev. D **77**, 054028 (2008).
[18] Z. G. He, Y. Fan, and K. T. Chao, Phys. Rev. D **75**, 074011 (2007).
[19] G. T. Bodwin, J. Lee, and C. Yu, Phys. Rev. D **77**, 094018 (2008).
[20] V. V. Braguta, Phys. Rev. D **79**, 074018 (2009).
[21] H.-R. Dong, F. Feng, and Y. Jia, Phys. Rev. D **85**, 114018 (2012).
[22] X.-H. Li and J.-X. Wang, arXiv:1301.0376.
[23] K. Wang, Y.-Q. Ma, and K.-T. Chao, Phys. Rev. D **84**, 034022 (2011).
[24] H. R. Dong, F. Feng, and Y. Jia, J. High Energy Phys. 10 (2011) 141.
[25] P. del Amo Sanchez *et al.* (*BABAR* Collaboration), Phys. Rev. D **82**, 011101 (2010).
[26] H. R. Dong, F. Feng, and Y. Jia, arXiv:1301.1946.
[27] R. Aaij *et al.* (LHCb Collaboration), Phys. Rev. Lett. **110**, 222001 (2013).
[28] Y. Jia, W.-L. Sang, and J. Xu, arXiv:1007.4541.
[29] Y. S. Kalashnikova and A. V. Nefediev, Phys. Rev. D **82**, 097502 (2010).

[30] Y.-B. Yang, Y. Chen, L.-C. Gui, C. Liu, Y.-B. Liu, Z. Liu, J.-P. Ma, and J.-B. Zhang, Phys. Rev. D **87**, 014501 (2013).
[31] T. J. Burns, F. Piccinini, A. D. Polosa, and C. Sabelli, Phys. Rev. D **82**, 074003 (2010) **87**, 034022 (2013).
[32] Y. Fan, J.-Z. Li, C. Meng, and K.-T. Chao, Phys. Rev. D **85**, 034032 (2012).
[33] S. J. Brodsky and G. P. Lepage, Phys. Rev. D **24**, 2848 (1981).
[34] G. T. Bodwin and A. Petrelli, Phys. Rev. D **66**, 094011 (2002).
[35] Y. Jia, X.-T. Yang, W.-L. Sang, and J. Xu, J. High Energy Phys. 06 (2011) 097.
[36] M. Beneke and V. A. Smirnov, Nucl. Phys. **B522**, 321 (1998).
[37] A. V. Smirnov, J. High Energy Phys. 10 (2008) 107.
[38] F. Feng, Comput. Phys. Commun. **183**, 2158 (2012).
[39] G. T. Bodwin, X. Garcia i Tormo, and J. Lee, Phys. Rev. Lett. **101**, 102002 (2008).
[40] M. A. Shifman and M. I. Vysotsky, Nucl. Phys. **B186**, 475 (1981).
[41] J. P. Ma and Z. G. Si, Phys. Lett. B **647**, 419 (2007).
[42] G. Bell and T. Feldmann, J. High Energy Phys. 04 (2008) 061.
[43] Y. Jia and D. Yang, Nucl. Phys. **B814**, 217 (2009).
[44] Y. Jia, J.-X. Wang, and D. Yang, J. High Energy Phys. 10 (2011) 105.
[45] Y. Jia, Phys. Rev. D **76**, 074007 (2007).
[46] B. Gong, Y. Jia, and J. X. Wang, Phys. Lett. B **670**, 350 (2009).
[47] J. Xu, H.-R. Dong, F. Feng, Y.-J. Gao, and Y. Jia, arXiv: 1212.3591.
[48] E. J. Eichten and C. Quigg, Phys. Rev. D **52**, 1726 (1995).
[49] W. Buchmüller and S.-H. H. Tye, Phys. Rev. D **24**, 132 (1981).
[50] C.-P. Shen (priviate communications).
[51] P. Pakhlov *et al.* (Belle Collaboration), Phys. Rev. D **79**, 071101 (2009).
[52] D. Binosi and L. Theussl, Comput. Phys. Commun. **161**, 76 (2004).
[53] D. Binosi, J. Collins, C. Kaufhold, and L. Theussl, Comput. Phys. Commun. **180**, 1709 (2009).
[54] W.-L. Sang and Y.-Q. Chen, Phys. Rev. D **81**, 034028 (2010).
[55] G. T. Bodwin, H. S. Chung, and J. Lee, Phys. Rev. D **90**, 074028 (2014).